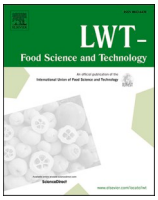
LWT - Food Science and Technology 228 (2025) 118058



Contents lists available at ScienceDirect

LWT

journal homepage: www.elsevier.com/locate/lwt





Antimicrobial coating for reusable produce-handling cardboard containers using clay complexed with a quaternary ammonium compound (QAC)

Yoonbin Kim [a,1], Hansol Doh [b,1], Nitin Nitin [a,c,*]

[a] Department of Food Science and Technology, University of California-Davis, Davis, CA, 95616, USA
[b] Department of Food Science and Biotechnology, Ewha Womans University, Seodaemun-gu, Seoul, 03760, Republic of Korea
[c] Department of Biological and Agricultural Engineering, University of California-Davis, Davis, CA, 95616, USA

ARTICLE INFO

Keywords:
Clay
Kaolin
Quaternary ammonium compound
Benzalkonium chloride
Antimicrobial coating
Cardboard box
Fresh produce

ABSTRACT

Bacterial cross-contamination of porous, reusable food packaging materials, such as cardboard, presents significant food safety challenges. Here, a novel antimicrobial coating system was developed using a combination of kaolin and benzalkonium chloride (BAC) for reusable cardboard boxes. A stable kaolin and BAC complex (kaolin@BAC) was formed through methoxylation of kaolin, followed by interactions between methoxylated kaolin and BAC, and uniformly deposited on the cardboard surface via a one-step paint-coating method. The kaolin@BAC-coated cardboard surface exhibited strong antimicrobial activities against bacterial cells and achieved > 4-log reductions of *Listeria innocua* and *Escherichia coli* O157:H7 cells within 15 min. The storage test revealed that the antimicrobial activity of the kaolin@BAC coating was retained for at least two weeks. Furthermore, the kaolin@BAC-coated cardboard significantly reduced the risk of produce-mediated cross-contamination, and only ca. 1.3 (detection limit) – 1.6 log CFU/cm^2 of *L. innocua* cells were enumerated from the coated surface after repeated exposure to contaminated cherry tomatoes, whereas ca. 3.8–4.4 log CFU/cm^2 of *L. innocua* cells were enumerated from non-coated cardboard surfaces. These findings highlight the potential of kaolin@BAC coatings as an effective strategy for reducing the bacterial cross-contamination of reusable food packaging materials, thereby enhancing the microbial safety of the food supply chain.

1. Introduction

Cardboard containers are widely used for the storage and transport of fresh produce and are often reused in packing houses and distribution facilities. Due to the porous nature of the cardboard material, there can be multiple sites for microbial harborage in these containers (Brandwein et al., 2016; Jin et al., 2021; Siroli et al., 2014). However, cardboard containers cannot be sanitized by conventional aqueous sanitation approaches commonly used for plastic totes and bins. Thus, reuse of cardboard poses a risk of bacterial cross-contamination during the packaging and transportation of fresh food products (Faour-Klingbeil et al., 2016; J. K. Kim & Harrison, 2008; Zeng et al., 2014). One potential strategy to reduce the risks of cross-contamination is to develop antimicrobial coatings on reusable packaging containers (DeFlorio et al., 2021; Doh & Nitin, 2022). However, most of the antimicrobial coating efforts have focused on non-porous materials, such as stainless steel and plastic (Clarke et al., 2017; Hage et al., 2021; Resnik et al., 2020), while limited efforts have been made to develop antimicrobial coatings on porous materials such as reusable cardboard box (CB) materials. Although various synthetic plastic-based polymers (e.g., polyvinyl chloride [PVC], polyethylene terephthalate [PET], polypropylene [PP], and polyethylene [PE] or bio-based polymers (e.g., alginate, beeswax, chitosan, cellulose, gelatin, and zein) have been applied as laminated coating layers for paper-based packaging, these coatings are primarily intended to enhance barrier properties against moisture, gases, and lipids rather than to impart active antimicrobial functionality (Dubowik et al., 2025; Lyytikäinen et al., 2025; Mujtaba et al., 2022; Resendiz-Diaz et al., 2025). Therefore, there is a need to develop a food-grade antimicrobial formulation that can be applied to porous surfaces, such as reusable CB, which are difficult to sanitize using conventional methods.

QACs are positively-charged surface-active agents with broad-spectrum antibacterial and antifungal activities (Bureš, 2019; Osimitz & Droege, 2021). Exposure to QACs increases the membrane permeability of the microbial cells, leading to cell lysis even at low

* Corresponding author. Department of Food Science and Technology, University of California-Davis, One Shields Avenue, Davis, CA, 95616, USA.
E-mail address: nnitin@ucdavis.edu (N. Nitin).
[1] These authors contributed equally to this paper.

https://doi.org/10.1016/j.lwt.2025.118058
Received 9 April 2025; Received in revised form 3 June 2025; Accepted 19 June 2025
Available online 20 June 2025
0023-6438/© 2025 The Authors. Published by Elsevier Ltd. This is an open access article under the CC BY license (http://creativecommons.org/licenses/by/4.0/).

concentrations (Osimitz & Droege, 2021; Saverina et al., 2023). QACs are considered relatively more stable and safer to use compared to other oxidizing sanitizers, such as peroxide- and chlorine-based sanitizers (Jones & Joshi, 2021; Lee & Pascall, 2020; Saverina et al., 2023). Due to these advantages, increasing efforts have been made to develop QAC-based antimicrobial coatings on food-handling surfaces (Min et al., 2020; Saverina et al., 2023). Many of these coating approaches involve binding of modified QACs to non-porous surfaces, such as silane-modified QACs on metal surfaces, or synthesizing polymers with cationic groups, such as quaternary ammonium salts, which are subsequently coated onto surfaces for antimicrobial activity (Lee & Pascall, 2020; Saverina et al., 2023). However, these modifications can significantly increase costs compared to conventional QACs used in the food industry, and in some cases, their application may be limited by regulatory constraints (Merchel Piovesan Pereira & Tagkopoulos, 2019; Osimitz & Droege, 2021). In addition, the depositions of these coatings on metal or plastic surfaces may require additional modifications of the substrate surface or the use of specialized coating equipment, which may not be readily accessible in food production environments including fresh produce packaging houses and distribution facilities. Furthermore, most of these studies have focused on non-porous metal or plastic surfaces, leaving a gap in understanding their efficacy on porous materials commonly found in food environments.

To address these challenges, this study develops and evaluates an antimicrobial coating for a porous, reusable CB material using a combination of clay complexed with benzyl ammonium chloride (BAC) to control the risk of cross-contamination. Kaolin was selected as a cost-effective and environmentally friendly clay material that can be deployed for food-contact applications, including food packaging (El Mouzahim et al., 2023; Rammak et al., 2021; Zhou et al., 2023). For the complexation of kaolin with BAC, kaolin was first modified to methoxy-kaolin, which interacted with BAC molecules through a combination of electrostatic adsorption and hydrophobic interactions, forming a stable kaolin-BAC complex (kaolin@BAC). Polyvinyl alcohol (PVA) was selected as a food-grade polymeric matrix and crosslinked with a food-grade crosslinker, maleic acid, to improve the distribution and adhesion of kaolin@BAC particles on CB surface. The physicochemical properties of kaolin@BAC coating were analyzed using X-ray photoelectron spectroscopy (XPS), infrared (IR) spectroscopy, thermogravimetric analysis (TGA), and scanning electron microscopy (SEM). The antimicrobial efficacy of the kaolin@BAC coating on the CB surface was evaluated using *Listeria innocua* and *E. coli* O157:H7 as model Gram-positive and Gram-negative bacteria, respectively. For the simulated cross-contamination test, cherry tomatoes were used as a model fresh produce. In addition, the storage stability of the coating on the CB surface was also evaluated. Overall, this study illustrates the development of a food-grade, clay-QACs-based antimicrobial coating to reduce bacterial cross-contamination of cardboard packaging materials in food-handling environments. Our approach is unique in that it can be directly applied to the existing porous cardboard surfaces without any pretreatment or modification of the substrate, or the use of specialized coating equipment.

2. Materials and methods

2.1. Materials

Kaolin, dimethyl sulfoxide (DMSO), methanol (MeOH; ACS reagent, ≥99 %), benzalkonium chloride (BAC), calcium carbonate ($CaCO_3$), polyvinyl alcohol (PVA; 30,000–70,000 Da, 87–89 % hydrolyzed), sodium thiosulfate ($Na_2S_2O_3$), maleic acid, maximum recovery diluent (MRD), and Tween 20 were purchased from Sigma-Aldrich (St. Louis, MO, USA). Luria-Bertani (L.B.) broth, tryptic soy broth (TSB), L.B. agar, rifampicin, tryptic soy agar (TSA), and phosphate-buffered saline (PBS; pH 7.4) were purchased from Thermo Fisher Scientific Inc. (Waltham, MA, USA). A reusable CB food packaging box and cherry tomatoes were obtained from the local market (Davis, CA, USA). Ultrapure water (18 MΩ cm) was prepared using the Milli-Q water ultra-purification system from EMD Millipore (Billerica, MA, USA).

2.2. Preparation of kaolin@BAC particles

The procedure for preparing kaolin@BAC consisted of three steps, as described in a previous report (Matusik & Kłapyta, 2013). First, 2 g of kaolin was immersed in a mixture of 27 mL of DMSO and 3 mL of deionized water (DW). The suspension was stirred constantly and heated at 70 °C for 2 h to activate the hydroxyl group on kaolin. The suspension was then centrifuged at 8800×*g* and dried at 60 °C for 48 h to remove the residual moisture from the particles. Next, 2 g of the activated kaolin was dispersed in 40 mL of MeOH at room temperature and stirred for 24 h to obtain methoxy-kaolin. The supernatant of the mixture was discarded after centrifuging at 8800×*g*, and the pelleted methoxy-kaolin particles were resuspended with fresh MeOH (40 mL). This procedure was repeated up to six times to increase the number of methoxy groups on methoxy-kaolin. After the methoxylation, the methoxy-kaolin particles were resuspended in 30 mL of DW, vortexed at the maximum speed for 60 s, and centrifuged at 8800×*g* before discarding the supernatant. The washing cycle was repeated up to three times to remove the residual MeOH from the methoxy-kaolin particles. Third, 0.2 g (wet basis) of methoxylated kaolin sample was mixed with 5 mL of 1.0 M BAC solution (prepared in MeOH). The suspension was then stirred at room temperature for 24 h, centrifuged, and the supernatant was discarded. The resulting kaolin@BAC particles were resuspended in 30 mL of DW, vortexed at the maximum speed for 60 s, and centrifuged at 8800×*g* before discarding the supernatant. This washing step was repeated three times to remove any residual BAC and MeOH from the kaolin@BAC particles. Finally, the kaolin@BAC particles were dried at 70 °C overnight to remove residual moisture from the particles. The kaolin@BAC particles were stored in a sealed container until further use.

2.3. Kaolin@BAC coating on the reusable cardboard box (CB)

For kaolin@BAC coating on the reusable CB, the kaolin@BAC particles were physically mixed with $CaCO_3$ at a ratio of 7:3 ($CaCO_3$:kaolin@BAC) using a magnetic stirrer for 10 min without a solvent. Then, DW and 10 % (v/v, diluted in DW) PVA solution were added and stirred for 30 min. After mixing, 60 % maleic acid was added to the mixture as a crosslinking agent for PVA and stirred for an additional 30 min. The bottom liner (inner surface) of the CB coupons was deposited with kaolin@BAC formulations using a paint-coating method, as described by Doh and Nitin (2022). After deposition, the kaolin@BAC-coated CB (kaolin@BAC-CB) was cured at 140 °C for 2 h and used for subsequent experiments. Plain CB and kaolin-coated CB without BAC (kaolin-CB) were used as control samples. The thickness of CB, kaolin-CB, and kaolin@BAC-CB samples was measured using a digital caliper with an accuracy of ±0.02 mm (General ULTRATech®, New York City, NY, USA). The coating thickness was calculated by subtracting the thickness of uncoated CB from that of the coated CB samples. Similarly, the coating weight was determined by measuring the weight difference between the uncoated and coated CB samples and expressed as weight per unit area (mg/cm^2).

2.4. Physcochemical characterization of kaolin@BAC coating

The physicochemical properties of kaolin@BAC coating were assessed based on its chemical structure, thermal stability, and morphological properties. First, the chemical structures of the kaolin@BAC coating were analyzed using X-ray photoelectron spectroscopy (XPS; PHI 5800 System with Monochromator, Ulvac-PHI, Inc., Chigasaki, Kanagawa, Japan) and attenuated total reflectance Fourier transform infrared spectroscopy (ATR-FTIR; Nicolet iS10, Thermo Fisher Scientific, Waltham, MA, USA). The kaolin@BAC particles were dried

overnight under ambient conditions before analysis. XPS was used to determine the surface chemical composition and bonding states of kaolin, BAC, and kaolin@BAC particles. Furthermore, chemical structure changes in kaolin@BAC particles were analyzed using an ATR-FTIR spectrometer in the range of 4000–500 cm^{-1}. The spectra were collected with 128 scans at a resolution of 4 cm^{-1} for each sample at a scan rate of 0.2 cm s^{-1}.

The thermal stability of kaolin@BAC coating on CB was measured using a thermogravimetric analyzer (TGA; Model 2950, T.A. Instruments, New Castle, DE, USA). The onset temperature (T_{on}) and decomposition temperature (T_d) of CB, Kaolin-CB, and kaolin@BAC-CB were determined at a heating rate of 10 °C/min from 25 °C to 600 °C under a nitrogen environment. Each sample was cut into fine pieces (ca. 5 mg) and loaded onto an aluminum sample pan for alanysis.

The morphological properties of kaolin@BAC particles, CB, and kaolin@BAC-CB were assessed using a scanning electron microscope (SEM; Thermo Fisher Quattro S, Thermo Fisher Scientific, Inc., Waltham, MA, USA). The SEM was operated at an accelerating voltage of 20.0 kV with a spot size of 2.5. The coated samples were sputter-coated with gold under vacuum for 2 min. SEM images were collected at magnifications ranging from 500× to 10,000 × .

2.5. Bacterial strains and inoculum preparation

The bacterial strains of rifampicin-resistant *Listeria innocua* (TVS451) and rifampicin-resistant *Escherichia coli* O157:H7 (ATCC 700728) were selected as models for Gram-positive and Gram-negative bacteria, respectively (Kim et al., 2024). A stock of cryo-preserved *L. innocua* and *E. coli* O157:H7 cells were streaked onto TSA plates and grown overnight at 37 °C. A single colony of *L. innocua* or *E. coli* O157:H7 cells was selected from the TSA plates and inoculated in the TSB. Then, the bacterial inoculated suspensions of TSB were incubated at 37 °C with constant shaking at 250 rpm overnight (ca. 15–18 h) to achieve the stationary phase cultures (ca. 9.3 log CFU/mL). The overnight L. *innocua* or *E. coli* O157:H7 culture was harvested, washed twice with PBS, and resuspended in PBS to prepare a bacterial inoculum for antimicrobial and cross-contamination studies.

2.6. Antimicrobial activity of kaolin@BAC-CB

The antimicrobial activities of kaolin@BAC-CB were evaluated against *L. innocua* and *E. coli* O157:H7. A 10 μL of bacterial suspension (ca. 8.3 log CFU/mL) was spot-inoculated onto the surface of kaolin@BAC-CB (1 × 1 cm^2) and incubated at room temperature for up to 30 min. Bacterial cells treated on CB (no coating) and kaolin-CB (no BAC) were included as controls. After incubation, the CB coupon was transferred to a 50 mL tube containing 10 mL of MRD supplemented with 0.1 % (v/v) Tween 20 and 0.1 M sodium thiosulfate. Sodium thiosulfate was used as a neutralizer for the residual BAC (Kovač et al., 2022). After 2 min of incubation, the mixture was vortexed vigorously for 1 min. The bacterial populations recovered from the CB surfaces were enumerated using a plate count assay. The bacterial suspensions were serially diluted in PBS, surface-plated on TSAR, and incubated at 37 °C for 48 h before counting the colonies. The theoretical detection limit of the plate count assay was 1.0 log CFU/cm^2.

2.7. Storage stability of kaolin@BAC-CB

The storage stability of kaolin@BAC-CB was evaluated by monitoring its antimicrobial activities during storage. Freshly prepared kaolin@BAC-CB was stored at room temperature in the dark for up to two weeks. After 0, 1, and 2 weeks of storage, the antimicrobial activities of kaolin@BAC-CB were evaluated against *L. innocua* and *E. coli* O157:H7 following the procedures described in section 2.6.

2.8. Cross-contamination test on kaolin@BAC-CB

The cherry tomato (*Solanum lycopersicum* var. *cerasiforme*) was selected as a model fresh produce for the cross-contamination test. The cherry tomatoes were rinsed with sterilized Milli-Q water before use. Then, the cherry tomatoes were dip-inoculated in 10 mL of *L. innocua* or *E. coli* O157:H7 suspensions (ca. 10^8 CFU/mL) and air-dried at room temperature for 1 h. To remove loosely bound bacterial cells, the inoculated cherry tomatoes were gently washed in 20 mL of sterilized Milli-Q water and air-dried at room temperature for 1 h. The contaminated cherry tomato was then placed in between two kaolin@BAC-CB coupons (2 × 2 cm^2) to maintain the consistent surface area of contact and incubated for up to 30 min (cycle 1). The process was repeated for up to 3 cycles, and the interval between each cycle was less than 1 min. A schematic of the cross-contamination test is illustrated in Fig. 4a. After three cycles of contact, the bacterial cells on the surfaces were recovered and enumerated following the procedures described in section 2.6. The theoretical detection limit of the plate count assay was 1.4 log CFU/cm^2.

2.9. Statistical analysis

All experiments were performed in at least triplicate, and results are presented as mean ± standard deviation (SD). Mean values labeled with different letters in the graphs indicate statistically significant differences. Data were analyzed using one-way analysis of variance (ANOVA), followed by Duncan's multiple range test at a significance level of $p \leq 0.05$. Statistical analysis was performed using SPSS software (Version 25.0; SPSS Inc., Chicago, IL, USA).

3. Results and discussions

3.1. Physcochemical characterization of kaolin@BAC coating

The thickness and weight of the coating are summarized in Table 1. The physicochemical properties of kaolin@BAC coating were characterized using XPS, FTIR, TGA, and SEM, respectively (Fig. 1). The chemical structural changes during the complexation process were assessed using XPS and FTIR spectroscopy, respectively (Fig. 1a and b). As shown in Fig. 1a, the XPS spectra of kaolin, BAC, and kaolin@BAC particles exhibited distinct surface compositions, primarily the oxygen group in kaolin and the carbon group in BAC. The peak at 531 eV, which corresponds to oxygen (O 1*s*), was observed in kaolin and kaolin@BAC spectra but not in BAC spectra. Also, the intensity of the oxygen peak in the kaolin@BAC particle was significantly reduced compared to native kaolin, suggesting the chemical interaction of kaolin and BAC. It has been reported that MeOH treatment of kaolin can induce the formation of methoxy groups (-O-CH_3), which can further facilitate hydrophobic interactions between the MeOH-treated kaolin and BAC (Matusik & Kłapyta, 2013). In addition, the presence of a C 1*s* peak at 280 eV in the kaolin@BAC spectra supports the formation of the complexed structure, as no C 1s peak was observed in kaolin, while BAC exhibited a strong C 1s peak. In addition, the peak changes in kaolin@BAC particles at 155, 120, 103, and 77 eV, corresponding to Si 2*s*, Al 2*s*, Si 2*p*, and Al 2*p*, respectively, further support the potential interactions between MeOH-treated kaolin and BAC, as reduced peak intensities were observed from kaolin@BAC compared to the native kaolin spectra.

Table 1
Thickness and weight of the coating.

	Thickness (mm)	Coating thickness (mm)	Coating weight (mg/cm2)
CB	2.44 ± 0.55	–	–
Kaolin-CB	3.10 ± 0.14	0.66 ± 0.47	116.10 ± 12.72
Kaolin@BAC-CB	3.26 ± 0.90	0.82 ± 0.46	122.30 ± 16.83

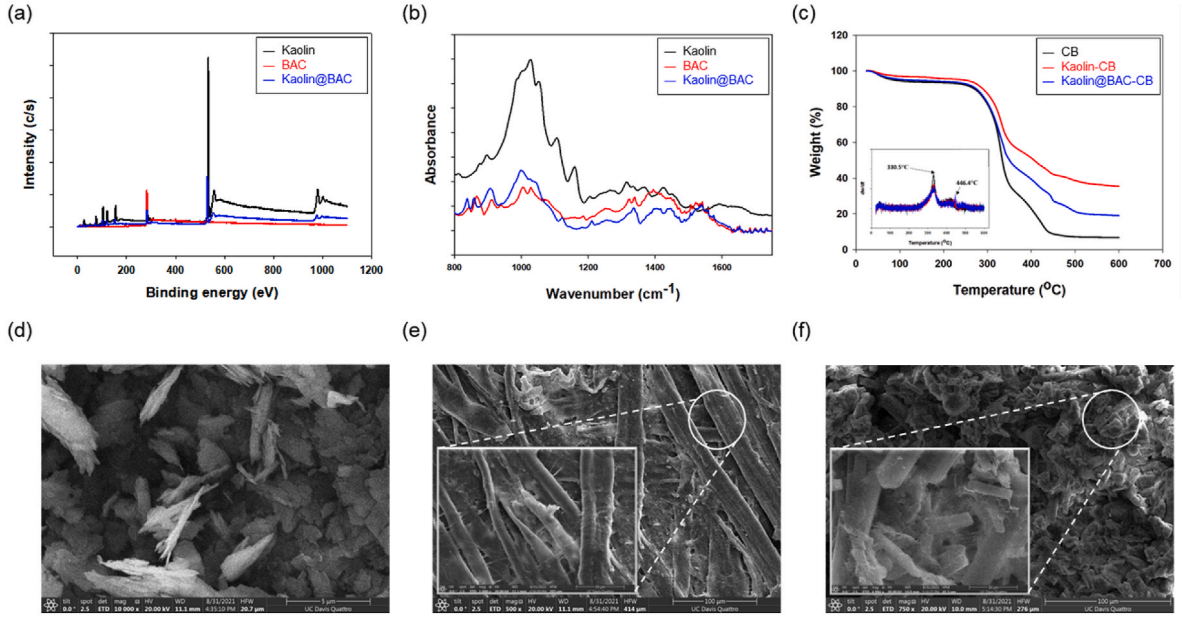


Fig. 1. Physicochemical characterization of kaolin@BAC coating. Methoxylated kaolin particles complexed with BAC were deposited on a cardboard surface using a paint-coating method. (a) XPS spectra of kaolin, BAC, and kaolin@BAC particles; (b) FTIR spectra of kaolin, BAC, and kaolin@BAC particles; (c) TGA curve of CB, kaolin-CB, and kaolin@BAC-CB; Representative SEM images of (d) kaolin@BAC particles at 10,000 × magnification (scale bar: 5 μm), (e) CB at 500 × magnification (scale bar: 100 μm) with an inset at 100 × magnification (scale bar: 50 μm), and (f) kaolin@BAC-CB at 500 × magnification (scale bar: 100 μm) with an inset at 100 × (scale bar: 50 μm).

The FTIR spectra of kaolin, BAC, and kaolin@BAC particles are shown in Fig. 1b. The main spectral changes are observed at 1009 cm^{-1}, 1396 cm^{-1}, and 1540 cm^{-1}. The *Si*-O stretching at 1009 cm^{-1} in kaolin is a main peak that is attributed to the backbone structure of the kaolin. As shown in Fig. 1b, the intensity of the peak at 1009 cm^{-1} was significantly reduced in kaolin@BAC compared to those of the native kaolin. This may be attributed to the reduced number of *Si*-O groups on kaolin surface upon treatment with MeOH, followed by complexation with BAC. In addition, the presence of C=C stretching bands in the kaolin@BAC spectra at 1396 cm^{-1} and 1540 cm^{-1}, corresponding to the benzene ring of BAC, further support the chemical interactions of BAC with kaolin, as no peaks were observed in the spectra of native kaolin at these spectral wavelengths.

Kaolin@BAC coating was deposited on CB, using $CaCO_3$, PVA, and maleic acid as the filler, binder, and cross-linking agent, respectively. This coating composition was easily deposited on the CB surface using a simple paint-coating method. CB (without coating) and Kaolin-PVA coating without BAC (kaolin-CB) were included as controls. The thermal stability of CB, kaolin-CB, and kaolin@BAC-CB are assessed using TGA, and the onset temperature (T_{on}) and decomposition temperature (T_d) were determined (Fig. 1c). Briefly, T_{on} was determined based on the intersection of the tangent to the TGA curve at the point of maximum temperature gradient and the extrapolated mass baseline. T_d was determined by the DTG curve (1st derivative of the TGA curve) as the temperature at which the highest mass loss rate of the sample was observed. For the CB samples, the onset of thermal decomposition was initiated at 272.8 °C, and the T_d was measured to be 330.5 °C, respectively. These results are consistent with the previous results reported for the CB material (Zhou et al., 2013). The authors reported that a significant mass loss was observed at temperatures between 250 °C and 375 °C, attributed to the pyrolysis of cellulose. In the cases of kaolin-CB and kaolin@BAC-CB, the second T_d for both samples was observed at 446.4 °C. This higher decomposition temperature may be attributable to the release of water molecules trapped in the interlayer structure of kaolin, which occurs between 300 °C and 500 °C (Panda et al., 2010).

Fig. 1d - f illustrate the SEM images of kaolin@BAC particles, CB, and kaolin@BAC-CB, respectively. As illustrated in Fig. 1d, kaolin@BAC particles formed needle-like structures with a length of ca. 5 μm and a width of ca. 0.4 μm. Kaolin@BAC particles exhibited a distinct morphology compared to that of kaolin and BAC, respectively (Supplementary Figure 1), indicating structural changes upon complexation of BAC with kaolin. The uncoated cardboard (CB) exhibited a porous network with long fiber structures (Fig. 1e) (Barbash & Yashchenko, 2020; Lavoine et al., 2014). Fig. 1f shows the kaolin@BAC coating deposited on the CB surface. No fiber structures of the CB were observed on the coated surfaces, suggesting the uniform distribution of the kaolin@BAC coating throughout the CB surface using the paint-coating method.

Overall, these findings suggest the physicochemical changes of kaolin upon methoxylation, followed by complexation with BAC particles. The XPS and FTIR analyses confirmed the chemical interactions between kaolin and BAC, while TGA results demonstrated improved thermal stability of the coated CB. Additionally, SEM images indicated distinct morphological changes in kaolin@BAC and a uniform coating on the CB surface. These results highlight the potential of kaolin@BAC coatings for enhancing the structural and thermal properties of coated materials.

3.2. Antimicrobial activities kaolin@BAC-CB

The antimicrobial activity of kaolin@BAC-CB was evaluated against *L. innocua* (Gram-positive) and *E. coli* O157:H7 (Gram-negative), respectively. As shown in Fig. 2a and b, a significant reduction (>4 log CFU/cm^2) of the bacterial populations was observed within 15 min of contact with the kaolin@BAC-CB. In contrast, bacterial cells treated on uncoated CB and kaolin-CB showed no significant reduction even after 30 min. A number of studies have reported the antimicrobial activity of BAC at varying concentrations against diverse bacterial pathogens. For example, Tezel et al. (2009) demonstrated that *Vibrio fischeri* was effectively inactivated within 5–15 min of BAC treatment at 0.2–1.0 mg/L. Thomas et al. (2005) reported ca. 4–5 log reduction of *Pseudomonas aeruginosa* within 5 min of BAC treatment at 60 mg/L. However, only a limited number of studies have demonstrated the antimicrobial potential of clay-BAC compositions for food packaging applications.

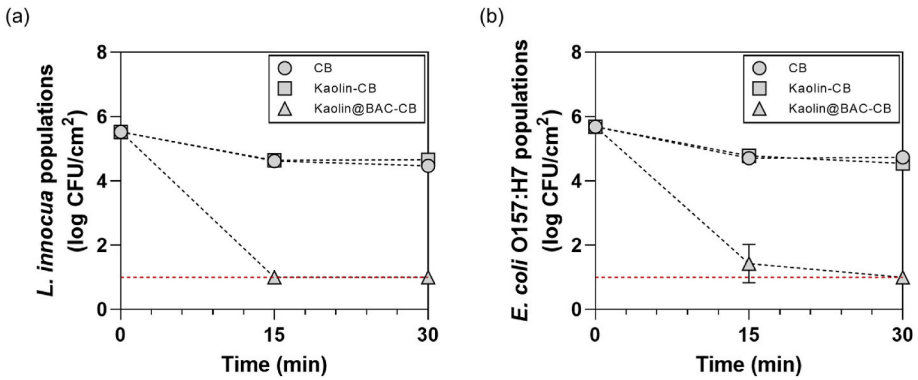


Fig. 2. Antimicrobial activities of kaolin@BAC-CB against (a) *L. innocua* and (b) *E. coli* O157:H7. Bacterial cells were incubated on CB, kaolin-CB, and kaolin@BAC-CB surface for up to 30 min, and bacterial populations were recovered from the surfaces and enumerated using a plate count assay. The theoretical detection limit of direct plating was 1.0 log CFU/cm^2 (red dashed line). The results represent the mean values and their standard deviations (n = 3).

Recently, the antimicrobial activities of the PVA films doped with kaolinite-BAC complexes have been demonstrated by Zhang et al. (2023). The authors reported that PVA films incorporated with kaolinite-BAC (30 % [w/w] of PVA) exerted limited antibacterial activities, forming a clear inhibition zone (ca. 11.3 mm) against *Staphylococcus aureus*. However, the kaolin-BAC antimicrobial composition developed in the present study is unique it that it was prepared as a coating formulation that can be applied directly to existing food-contact surfaces via a paint coating method, exerting enhanced antimicrobial activities compared to the previous study. To the best of knowledge, the antimicrobial activity of clay-BAC complexes within a PVA coating matrix has not been demonstrated for food packaging materials, including those with porous surfaces.

3.3. Storage stability of kaolin@BAC-CB

The antimicrobial properties of kaolin@BAC coating on CB surface were evaluated during a two-week storage period. Fig. 3 shows the antimicrobial efficacy of the kaolin@BAC-CB samples against *L. innocua* (Fig. 3a) and *E. coli* O157:H7 (Fig. 3b) after 0, 1, and 2 weeks of storage. Both bacterial populations decreased below the detection limit (1.0 log CFU/cm^2) after 30 min of incubation on one-week-old kaolin@BAC-CB. In adition, only ca. 1.0–1.2 log CFU/cm^2 bacterial cells were enumerated from the two-weeks-old kaolin@BAC-CB after 30 min of incubation, without showing any significant differences compared to the freshly prepared kaolin@BAC-CB (0-week-old). These results indicate that kaolin@BAC coating can provide persistent antimicrobial activities on the CB surface for an extended period.

The storage stability of BAC-based antimicrobial coating has been reported by others. For example, Lee and Pascall (2020) reported that silane-QAC coated metal surfaces exerted significant antimicrobial activities even after 3 months of storage, achieving >5 log reductions of *L. innocua* cells and 3–4 log reductions of *E. coli* cells within 24 h of treatment. Furthermore, Jung et al. (2019) reported that quaternary ammonium chitosan/sodium alginate multilayer coatings formed on poly (methyl methacrylate) (PMMA)-based denture materials retained their antibiofilm activities even after 4 weeks of storage in PBS. These findings highlight the potential of QACs as a stable agent that can be incorporated into a coating matrix, exhibiting long-term antimicrobial activities. To the best of our knowledge, the storage stability of clay-BAC coating on a porous cardboard surface has not been reported.

3.4. Prevention of bacterial cross-contamination

The effectiveness of kaolin@BAC coating in preventing the bacterial cross-contamination of CB was tested using cherry tomatoes. Cherry tomatoes inoculated with bacterial cells were shake-incubated in a CB box coated with kaolin@BAC for 30 min, and the procedure was repeated for up to 3 cycles. Fig. 4 illustrates that a significantly lower number of bacterial cells were enumerated from kaolin@BAC-CB surface compared to CB and kaolin-CB. For example, ca. 3.8–4.4 and 4.2–4.8 log CFU/cm^2 of *L. innocua* cells were enumerated from CB and kaolin-CB, respectively, whereas only ca. 1.3 (detection limit) – 1.6 log CFU/cm^2 of *L. innocua* cells were enumerated from kaolin@BAC-CB during cross-contamination cycles. Notably, no significant increase in the bacterial populations was observed from kaolin@BAC-CB across

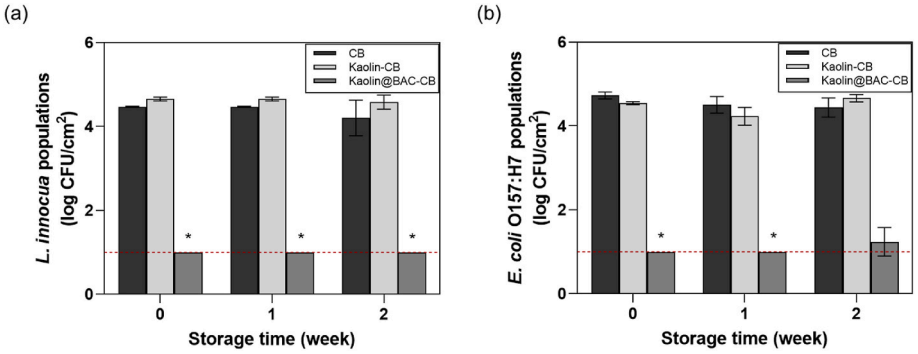


Fig. 3. Storage stability of kaolin@BAC-CB. Kaolin@BAC-CB was stored at room temperature in the dark for up to two weeks, and its antimicrobial activities were evaluated against (a) *L. innocua* and (b) *E. coli* O157:H7, respectively. Bacterial cells were incubated on CB, kaolin-CB, and kaolin@BAC-CB surface for 30 min, and bacterial populations were recovered from the surfaces and enumerated using a plate count assay. The theoretical detection limit of direct plating was 1.0 log CFU/cm^2 (red dashed line). The results represent the mean values and their standard deviations (n = 3), and the asterisks indicate that the number of bacteria was below the detection limit.

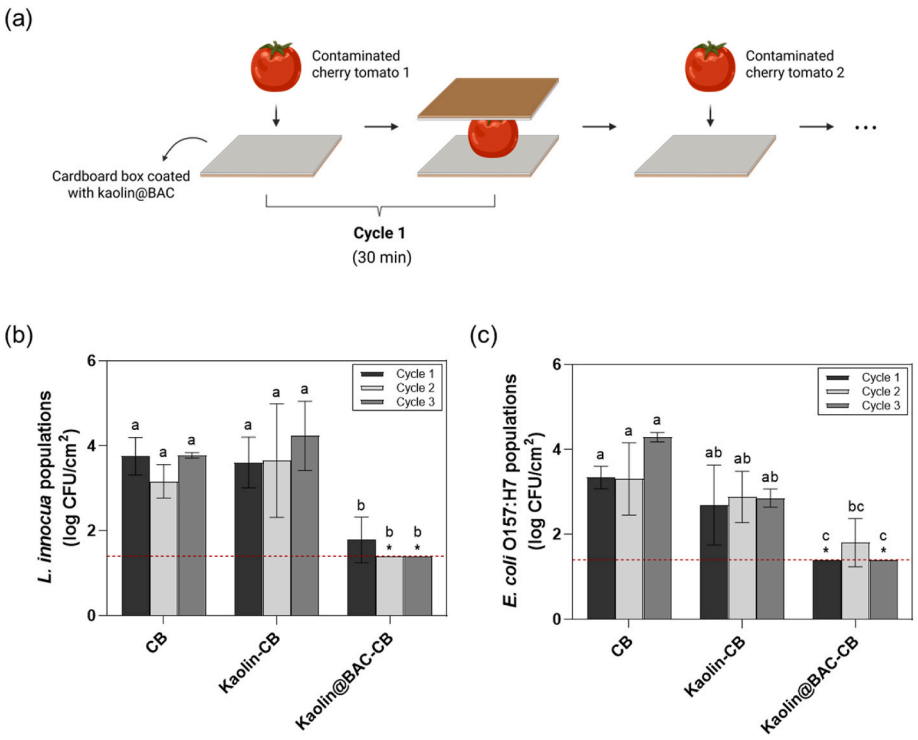


Fig. 4. Inhibition of produce-mediated bacterial cross-contamination of cardboard using kaolin@BAC coating: (a) Schematic of the simulated cross-contamination study. CB, kaolin-CB, and kaolin@BAC-CB were repeatedly contacted with cherry tomatoes contaminated with *L. innocua* for 30 min per cycle, up to three cycles. Bacterial populations on the surfaces were recovered and enumerated using a plate count assay, and the theoretical detection limit of direct plating was ca. 1.4 log CFU/cm^2 (red dashed line). The results represent the mean values and their standard deviations ($n = 3$), and different lowercase letters indicate statistically significant differences ($p < 0.05$). The asterisks indicate that the number of bacteria was below the detection limit.

repeated cross-contamination cycles. These results indicate that kaolin@BAC-CB effectively inhibited the bacterial cross-contamination of the CB surface, exhibiting strong self-cleaning potential.

The potential of QAC-based antimicrobial coatings has been extensively explored for non-porous food-contact surfaces. For example, Dong et al. (2021) demonstrated that phosphonate/QAC copolymer coating deposited on metal surfaces exhibited up to 99.4 % (ca. 2.2 log reduction) and 98.8 % (ca. 1.9 log reduction) of inhibition against *E. coli* and *Staphylococcus aureus*, respectively, after 8 h of contact. Similarly, Min et al. (2020) reported that the QAC-modified chitosan and PVA-based composite film reduced *E. coli* and *S. aureus* populations by up to 99.7 % (ca. 2.5 log reduction) and 98.5 % (ca. 1.8 log reduction), respectively, after 24 h of incubation. In the shelf-life study, strawberries coated with the composite films showed significantly reduced decay over 5 days of storage at 25 °C. However, to the best of knowledge, the potential of QAC-based coatings for preventing surface-mediated cross-contamination on porous food-contact surfaces has not been previously demonstrated.

Furthermore, it is also noteworthy that the kaolin@BAC-CB exhibited significantly enhanced antimicrobial activities, showing more than 4 log reductions of bacterial cells within 15 min of contact (Fig. 2). The strong antimicrobial activities of kaolin@BAC-CB may be attributed to the enhanced stability of BAC upon complexation with the kaolin matrix, potentially via hydrophobic and electrostatic interactions. It is possible that the stabilization of BAC may have reduced nonspecific interactions with the food matrix and limited its potential depletion, thereby contributing to consistent antimicrobial activity over repeated exposure cycles (Qiu et al., 2024; Wang et al., 2024; Yao et al., 2024). In addition, the inherent affinity of kaolin particles to bind bacterial cells may have facilitated the direct contact between BAC molecules and bacterial celsls, leading to membrane disruption and lysis (Abdel-Khalek et al., 2014; Joo et al., 2023). The porous microstructure and high surface area of the kaolin matrix may have resulted in increased available contact sites for BAC to interact with bacterial cells.

4. Conclusions

This study demonstrated the development of a novel antimicrobial coating system using kaolin and benzalkonium chloride (BAC) for reusable cardboard packaging. XPS and FTIR spectra and the TGA curve revealed that a stable kaolin and BAC complex (kaolin@BAC) was formulated through the methoxylation of kaolin, followed by complexation with BAC. SEM images demonstrated the morphological changes induced on kaolin@BAC particles and on cardboard surface with kaolin@BAC coating. The kaolin@BAC-coated cardboard surface exhibited strong antimicrobial activities against bacterial cells, achieving > 4-log reductions of *L. innocua* and *E. coli* O157:H7 cells within 15 min of contact. The antimicrobial activity of the coated cardboard was retained for at least two weeks. In addition, the kaolin@BAC coating significantly reduced the risk of produce-mediated cross-contamination of the cardboard surfaces. About 1.3 (detection limit) – 1.6 log CFU/cm^2 of *L. innocua* cells were enumerated from the coated cardboard surface after repeated exposure to contaminated cherry tomatoes, whereas ca. 3.8–4.4 CFU/cm^2 of *L. innocua* cells were enumerated from the non-coated cardboard surfaces. These findings provide novel insights into the development of an effective antimicrobial intervention for reusable, porous food packaging materials. The combination of clay and QAC-based antimicrobial coatings presents a practical strategy for enhancing food safety and minimizing cross-contamination risks in fresh produce supply chains. In future studies, bioanalytical approaches such as transcriptomics and metabolomics are needed to elucidate the molecular mechanisms underlying the antimicrobial activity of kaolin@BAC coatings. In addition, the potential for further optimization of the kaolin@BAC coating should be evaluated through systematic screening of various combinations of food-grade polymeric binders and cross-linkers, with a focus on improving mechanical durability under

physical and chemical stresses. Moreover, future studies should focus on establishing reliable analytical methods, such as LC-MS or HPLC, to quantify surface-available and total QAC content in clay-based carriers for a more accurate assessment of their antimicrobial efficacy and structural stability. The potential chemical migration and long-term stability of QACs on porous cardboard surfaces should be evaluated to ensure regulatory compliance and facilitate the translation of the developed antimicrobial coating approach.

CRediT authorship contribution statement

Yoonbin Kim: Writing – review & editing, Writing – original draft, Visualization, Validation, Project administration, Methodology, Investigation, Formal analysis, Conceptualization. **Hansol Doh:** Writing – review & editing, Writing – original draft, Visualization, Validation, Project administration, Methodology, Investigation, Formal analysis, Conceptualization. **Nitin Nitin:** Writing – review & editing, Supervision, Resources, Project administration, Methodology, Funding acquisition, Conceptualization.

Declaration of competing interest

The authors declare that they have no known competing financial interests or personal relationships that could have appeared to influence the work reported in this paper.

Acknowledgement

This research was supported by the USDA-NIFA Foundational Food Safety Program grant (2022-67017-36308) and the Center for Produce Safety grant (2021CPS08). This research was also supported by the National Research Foundation of Korea (NRF) grant funded by the Ministry of Science and ICT (MSIT) (RS-2023-00248098).

Appendix A. Supplementary data

Supplementary data to this article can be found online at https://doi.org/10.1016/j.lwt.2025.118058.

Data availability

Data will be made available on request.

References

Barbash, V. A., & Yashchenko, O. V. (2020). Preparation and application of nanocellulose from non-wood plants to improve the quality of paper and cardboard. *Applied Nanoscience, 10*(8), 2705–2716. https://doi.org/10.1007/s13204-019-01242-8

Brandwein, M., Al-Quntar, A., Goldberg, H., Mosheyev, G., Goffer, M., Marin-Iniesta, F., López-Gómez, A., & Steinberg, D. (2016). Mitigation of biofilm formation on corrugated cardboard fresh produce packaging surfaces using a novel thiazolidinedione derivative integrated in acrylic emulsion polymers. *Frontiers in Microbiology, 7*, 159. https://doi.org/10.3389/fmicb.2016.00159

Bureš, F. (2019). Quaternary ammonium compounds: Simple in structure, complex in application. *Topics in Current Chemistry, 377*(3), 14. https://doi.org/10.1007/s41061-019-0239-2

Clarke, D., Tyuftin, A. A., Cruz-Romero, M. C., Bolton, D., Fanning, S., Pankaj, S. K., Bueno-Ferrer, C., Cullen, P. J., & Kerry, J. P. (2017). Surface attachment of active antimicrobial coatings onto conventional plastic-based laminates and performance assessment of these materials on the storage life of vacuum packaged beef sub-primals. *Food Microbiology, 62*, 196–201. https://doi.org/10.1016/j.fm.2016.10.022

DeFlorio, W., Liu, S., White, A. R., Taylor, T. M., Cisneros-Zevallos, L., Min, Y., & Scholar, E. M. (2021). Recent developments in antimicrobial and antifouling coatings to reduce or prevent contamination and cross-contamination of food contact surfaces by bacteria. *Comprehensive Reviews in Food Science and Food Safety, 20*(3), 3093–3134. https://doi.org/10.1111/1541-4337.12750

Doh, H., & Nitin, N. (2022). Gelatin-based rechargeable antibacterial hydrogel paint coating for reducing cross-contamination and biofilm formation on stainless steel. *Food Control, 141*, Article 109113. https://doi.org/10.1016/j.foodcont.2022.109113

Dubowik, M., Przybysz, K., Dańczak, J., Lipkiewicz, A., Gajadhur, M., Górska, B., … Przybysz, P. (2025). Micro-and nanofibrillated cellulose coatings as barriers against water and oil in food packaging paper: A sustainable alternative to plastic coatings. *Coatings, 15*(3), 270. https://doi.org/10.3390/coatings15030270

El Mouzahim, M., Eddarai, E. M., Eladaoui, S., Guenbour, A., Bellaouchou, A., Zarrouk, A., & Boussen, R. (2023). Food packaging composite film based on chitosan, natural kaolinite clay, and *Ficus carica* leaves extract for fresh-cut apple slices preservation. *International Journal of Biological Macromolecules, 233*, Article 123430. https://doi.org/10.1016/j.ijbiomac.2023.123430

Faour-Klingbeil, D., Murtada, M., Kuri, V., & Todd, E. C. (2016). Understanding the routes of contamination of ready-to-eat vegetables in the Middle East. *Food Control, 62*, 125–133. https://doi.org/10.1016/j.foodcont.2015.10.024

Hage, M., Akoum, H., Chihib, N. E., & Jama, C. (2021). Antimicrobial peptides-coated stainless steel for fighting biofilms formation for food and medical fields: Review of literature. *Coatings, 11*(10), 1216. https://doi.org/10.3390/coatings11101216

Jin, K., Tang, Y., Liu, J., Wang, J., & Ye, C. (2021). Nanofibrillated cellulose as coating agent for food packaging paper. *International Journal of Biological Macromolecules, 168*, 331–338. https://doi.org/10.1016/j.ijbiomac.2020.12.066

Jones, I. A., & Joshi, L. T. (2021). Biocide use in the antimicrobial era: A review. *Molecules, 26*(8), 2276. https://doi.org/10.3390/molecules26082276

Jung, J., Li, L., Yeh, C. K., Ren, X., & Sun, Y. (2019). Amphiphilic quaternary ammonium chitosan/sodium alginate multilayer coatings kill fungal cells and inhibit fungal biofilm on dental biomaterials. *Materials Science and Engineering: C, 104*, Article 109961. https://doi.org/10.1016/j.msec.2019.109961

Kim, J. K., & Harrison, M. A. (2008). Transfer of *Escherichia coli* O157:H7 to romaine lettuce due to contact water from melting ice. *Journal of Food Protection, 71*(2), 252–256. https://doi.org/10.4315/0362-028X-71.2.252

Kim, Y., Zhao, H., Avena-Bustillos, R. J., Wang, S. C., & Nitin, N. (2024). Synergistic antimicrobial activities of aqueous extract derived from olive byproduct and their modes of action. *Chemical and Biological Technologies in Agriculture, 11*(1), 122. https://doi.org/10.1186/s40538-024-00634-5

Kovač, B., Piletić, K., Kovačević Ganić, N., & Gobin, I. (2022). The effectiveness of benzalkonium chloride as an active compound on selected foodborne pathogens biofilm. *Hygie, 2*(4), 226–235. https://doi.org/10.3390/hygiene2040020

Lavoine, N., Bras, J., & Desloges, I. (2014). Mechanical and barrier properties of cardboard and 3D packaging coated with microfibrillated cellulose. *Journal of Applied Polymer Science, 131*(8), Article 40106. https://doi.org/10.1002/app.40106

Lee, J., & Pascall, M. A. (2020). Reduction in microbial survival on food contact surfaces by a spray coated polymerized quaternary ammonium compound. *Food Science and Nutrition, 8*(5), 2472–2477. https://doi.org/10.1002/fsn3.1537

Lyytikäinen, J., Koljonen, K., & Leminen, V. (2025). Effects of multilayered cellulose-based coatings on the barrier properties of paperboard. *Cellulose*, 1–12. https://doi.org/10.1007/s10570-025-06416-y

Matusik, J., & Kłapyta, Z. (2013). Characterization of kaolinite intercalation compounds with benzylalkylammonium chlorides using XRD, TGA/DTA and CHNS elemental analysis. *Applied Clay Science, 83*, 433–440. https://doi.org/10.1016/j.clay.2013.07.019

Merchel Piovesan Pereira, B., & Tagkopoulos, I. (2019). Benzalkonium chlorides: Uses, regulatory status, and microbial resistance. *Applied and Environmental Microbiology, 85*(13), Article e00377. https://doi.org/10.1128/AEM.00377-19, 19.

Min, T., Zhu, Z., Sun, X., Yuan, Z., Zha, J., & Wen, Y. (2020). Highly efficient antifogging and antibacterial food packaging film fabricated by novel quaternary ammonium chitosan composite. *Food Chemistry, 308*, Article 125682. https://doi.org/10.1016/j.foodchem.2019.125682

Mujtaba, M., Lipponen, J., Ojanen, M., Puttonen, S., & Vaittinen, H. (2022). Trends and challenges in the development of bio-based barrier coating materials for paper/cardboard food packaging; a review. *Science of the total environment, 851*, Article 158328. https://doi.org/10.1016/j.scitotenv.2022.158328

Osimitz, T. G., & Droege, W. (2021). Quaternary ammonium compounds: Perspectives on benefits, hazards, and risk. *Toxicological Research and Application, 5*, Article 23978473211049085. https://doi.org/10.1177/23978473211049085

Panda, A. K., Mishra, B. G., Mishra, D. K., & Singh, R. K. (2010). Effect of sulphuric acid treatment on the physico-chemical characteristics of kaolin clay. *Colloids and Surfaces A: Physicochemical and Engineering Aspects, 363*(1–3), 98–104. https://doi.org/10.1016/j.colsurfa.2010.04.022

Qiu, Y. L., Li, Y., Zhang, G. L., Hao, H., Hou, H. M., & Bi, J. (2024). Quaternary-ammonium chitosan, a promising packaging material in the food industry. *Carbohydrate Polymers, 323*, Article 121384. https://doi.org/10.1016/j.carbpol.2023.121384

Rammak, T., Boonsuk, P., & Kaewtatip, K. (2021). Mechanical and barrier properties of starch blend films enhanced with kaolin for application in food packaging. *International Journal of Biological Macromolecules, 192*, 1013–1020. https://doi.org/10.1016/j.ijbiomac.2021.10.081

Resendiz-Diaz, B., Sadler, E., Schwikkard, S., Bear, J. C., & Crick, C. R. (2025). The fabrication of superhydrophobic coatings using food-grade wax dispersions. *Advanced Materials Interfaces.* , Article 2500106.. https://doi.org/10.1002/admi.202500106

Resnik, M., Benčina, M., Levičnik, E., Rawat, N., Iglič, A., & Junkar, I. (2020). Strategies for improving antimicrobial properties of stainless steel. *Materials, 13*(13), 2944. https://doi.org/10.3390/ma13132944

Saverina, E. A., Frolov, N. A., Kamanina, O. A., Arlyapov, V. A., Vereshchagin, A. N., & Ananikov, V. P. (2023). From antibacterial to antibiofilm targeting: An emerging paradigm shift in the development of quaternary ammonium compounds (QACs). *ACS Infectious Diseases, 9*(3), 394–422. https://doi.org/10.1021/acsinfecdis.2c00469

Siroli, L., Patrignani, F., Serrazanetti, D. I., Chiavari, C., Benevelli, M., Grazia, L., & Lanciotti, R. (2014). Antibacterial activity of biodegradable films incorporating

essential oils on foodborne pathogens. *Journal of Food Science, 79*(7), M1377–M1383. https://doi.org/10.1111/1750-3841.12439

Tezel, U., Giles, H., deRussy, A., & Pavlostathis, S. G. (2009). Effect of counter ions and natural organic matter on the toxicity of benzalkonium chloride. *Proceedings of the Water Environment Federation, 2009*(17), 621–631. https://doi.org/10.2175/193864709793955960

Thomas, L., Russell, A. D., & Maillard, J. Y. (2005). Antimicrobial activity of chlorhexidine diacetate and benzalkonium chloride against *Pseudomonas aeruginosa* and its response to biocide residues. *Journal of Applied Microbiology, 98*(3), 533–543. https://doi.org/10.1111/j.1365-2672.2004.02402.x

Wang, S., Qiu, B., Shi, J., & Wang, M. (2024). Quaternary ammonium antimicrobial agents and their application in antifouling coatings: A review. *Journal of Coatings Technology and Research, 21*(1), 87–103. https://doi.org/10.1007/s11998-023-00825-z

Yao, Y., Ye, Z., Zhang, Y., Wang, Y., & Yu, C. (2024). Quaternary ammonium compounds and their composites in antimicrobial applications. *Advanced Materials Interfaces, 11*(17), Article 2300946. https://doi.org/10.1002/admi.202300946

Zeng, W., Vorst, K., Brown, W., Marks, B. P., Jeong, S., Pérez-Rodríguez, F., & Ryser, E. T. (2014). Growth of *Escherichia coli* O157:H7 and *Listeria monocytogenes* in packaged fresh-cut romaine mix at fluctuating temperatures during commercial transport, retail storage, and display. *Journal of Food Protection, 77*(2), 197–206. https://doi.org/10.4315/0362-028X.JFP-13-117

Zhang, X., Li, S., Deng, Y., Zuo, Z., Sun, Z., Li, C., & Zheng, S. (2023). Benzalkonium chloride modified kaolinite with rapid bactericidal activity for the development of antibacterial films. *Materials Today Communications, 35*, Article 106152. https://doi.org/10.1016/j.mtcomm.2023.106152

Zhou, L., Hao, M., Min, T., Bian, X., Du, H., Sun, X., Zhu, Z., & Wen, Y. (2023). Kaolin incorporated with thyme essential oil for humidity-controlled antimicrobial food packaging. *Food Packaging and Shelf Life, 38*, Article 101106. https://doi.org/10.1016/j.fpsl.2023.101106

Zhou, C., Yang, W., & Blasiak, W. (2013). Characteristics of waste printing paper and cardboard in a reactor pyrolyzed by preheated agents. *Fuel Processing Technology, 116*, 63–71. https://doi.org/10.1016/j.fuproc.2013.04.023